# Cortex Segmentation - A Fast Variational Geometric Approach

Roman Goldenberg, Ron Kimmel, Ehud Rivlin, Michael Rudzsky
Computer Science Department
Technion—Israel Institute of Technology
Technion City, Haifa 32000, ISRAEL
E-mail: romang/ron/ehudr/rudzsky@cs.technion.ac.il
WWW home page: http://www.cs.technion.ac.il/∼ron

## Abstract

*An automatic cortical gray matter segmentation from a three-dimensional brain images (MR or CT) is a well known problem in medical image processing. In this paper we formulate it as geometric variational problem for propagation of two coupled bounding surfaces. An efficient numerical scheme is used to implement the geodesic active surface model. Experimental results of cortex segmentation on real three-dimensional MR data are provided.*

## 1. Introduction

The cerebral cortex is the outmost layer of the brain bounded by the outer cortical surface (Cerebral Spinal Fluid (CSF) – gray matter interface) and the inner cortical surface (gray matter – white matter interface). Determining the location of the cortical surface of the human brain is often a first step in brain visualization and analysis. Due to the complicated and convoluted nature of the cortex, the manual slice by slice segmentation is generally a difficult, inefficient and inaccurate process, which makes an automatic 3D cortex segmentation an important task.

A significant number of techniques have been proposed to deal with the problem. The whole set of approaches can be roughly divided into two groups: region based methods and boundary detection methods. Here we concentrate on one promising direction that is based on deformable surfaces. Deformable surface is a 3D analog of the active contour model that was introduced in [15, 30] as the 'snake model' and is based on minimizing an energy along a curve. Caselles et al. [3] and Malladi et al. [21] introduced a geometric flow that includes an internal and external geometric measures. Later, the geodesic active contour model derived from a re-parameterization invariant functional was proposed as a geometric alternative for the snakes [4, 5, 16, 27]. Efficient numerical methods were developed for accelerating of deformable surfaces propagation and some of them were applied for brain segmentation, e.g. see [20].

The idea to use several interacting deformable contours/surfaces for segmentation was exploited by several research teams. Samson et al. [24] proposed a supervised classification model to find an image partition composed of homogeneous regions, assuming the number of classes and their intensity properties are known. The classification problem was formulated using a variational framework aimed to propagate mutually exclusive regular curves towards class region boundaries. Paragios and Deriche [23] presented an image segmentation approach that incorporates boundary and region information sources under a curve-based minimization framework (see also [6] for a related effort). The propagating interfaces are coupled by demanding a non-overlapping set of curves that restricts each pixel to belong to only one region.

More recently, there has been an effort to apply constraints imposed by the cortex structure properties for better segmentation. Davatzikos et al. [11, 10] used the homogeneity of intensity levels within the gray matter region to introduce a force that would drive a deformable surface toward the center of the gray matter layer. Teo et al. [29] used the connectivity of the gray matter as a constraint in building the cortex representation by growing out from the white matter boundary. MacDonald et al. [18, 19] proposed to use an inter-surface proximity constraint in a two surface model of the inner and outer cortex boundaries in order to guarantee that surfaces do not intersect themselves or each other. Finally, Zeng et al. [33] used the fact that the cortical layer has a nearly constant thickness to design a coupled surfaces model in such a way that a special propagation speed term forces the inter-surface distance to remain within a predefined range.

In this paper we adopt the coupled surfaces model and develop it using a variational geometric framework. Our implementation is based on advanced numerical schemes

for surface evolution that yield a geometrically consistent and computationally efficient technique.

## 2. The Geometric-Variational Approach

### 2.1. Coupled surfaces segmentation as a minimization problem

Let $\mathcal{S}(u,v) : \mathbb{R}^2 \rightarrow \mathbb{R}^3 = (x(u,v), y(u,v), z(u,v))$ be a parameterized two-dimensional surface in 3-D space. Using the active contour approach, a boundary segmentation can be seen as a weighted area minimization problem

$$\min_{\mathcal{S}} \int g(x,y,z)da = \min_{\mathcal{S}} \int g(\mathcal{S}(u,v))|\mathcal{S}_u \times \mathcal{S}_v|dudv,$$

where $da$ is an area element and $g(x,y,z) : \mathbb{R}^3 \rightarrow \mathbb{R}^+$ is a positive boundary indicator function that depends on the image. It gets small, close to zero values along the boundary and higher values elsewhere.

In order to extract the cortical layer we have to find its two bounding surfaces: The outer CSF – gray matter interface, and the inner gray matter – white matter interface.

Theoretically, if one could provide perfect boundary indicator functions both for the inner and outer interfaces - $g_{in}()$ and $g_{out}()$ - it would have been sufficient to use a single surface approach, i.e. to find the inner and outer bounding surfaces $\mathcal{S}^{in}$ and $\mathcal{S}^{out}$ by separate minimization of the two uncoupled functionals

$$\mathcal{S}^{in} = \arg\min_{\mathcal{S}} \int g_{in}da, \quad \mathcal{S}^{out} = \arg\min_{\mathcal{S}} \int g_{out}da \quad (1)$$

In practice, the limitations imposed by the imaging devices often result in noisy and inaccurate image data, which reduce the reliability of boundary detectors that use only local information, e.g. voxel intensity, gradient, etc.

That is the main reason for incorporating additional constraints imposed by the nature of the problem. In the case of cortex segmentation it was suggested to use the fact that the cortical layer has a nearly constant thickness (about 3mm) [2]. Zeng et al. [33] designed a coupled surfaces model where two deformable surfaces are kept within a predefined normal range from each other by specially designing the interface propagation speed in such a way that it decreases whenever surfaces are getting too far or too close.

Let us adopt a similar coupled surfaces approach, but, rather than heuristically building an expression for the surface propagation speed [33], we shall derive it from a minimization problem. This time, unlike in (1), we want a simultaneous minimization of both interfaces $\mathcal{S}^{in}$ and $\mathcal{S}^{out}$, so that the minimum is reached when $\mathcal{S}^{in}$ captures the CSF – gray matter boundary and $\mathcal{S}^{out}$ locks on to the white matter – gray matter boundary. We start with

$$(\mathcal{S}^{in}, \mathcal{S}^{out}) = \arg\min_{\mathcal{S}^{in},\mathcal{S}^{out}} \left[ \int_{\mathcal{S}^{in}} g_{in}da + \int_{\mathcal{S}^{out}} g_{out}da \right]. \quad (2)$$

Motivated by [33] we link between the two surfaces, and introduce an additional component that penalizes the deviations of the inter-surface distance from the normal range, which yields the functional

$$\begin{aligned}
\mathcal{F}(\mathcal{S}^{in}, \mathcal{S}^{out}) &= \int_{\mathcal{S}^{in}} h\left[d((x,y,z), \mathcal{S}^{out})\right] g_{in}(x,y,z)da \\
&\quad + \int_{\mathcal{S}^{out}} h\left[d((x,y,z), \mathcal{S}^{in})\right] g_{out}(x,y,z)da \\
&= \int_{\mathcal{S}^{in}} h\left[d(\mathcal{S}^{in}(u,v), \mathcal{S}^{out})\right] g_{in}(\mathcal{S}^{in}(u,v)) \\
&\quad \cdot |\mathcal{S}^{in}_u \times \mathcal{S}^{in}_v|dudv \\
&\quad + \int_{\mathcal{S}^{out}} h\left[d(\mathcal{S}^{out}(u,v), \mathcal{S}^{in})\right] g_{out}(\mathcal{S}^{out}(u,v)) \\
&\quad \cdot |\mathcal{S}^{out}_u \times \mathcal{S}^{out}_v|dudv, \qquad (3)
\end{aligned}$$

where $d((x,y,z), \mathcal{S})$ is the Euclidean distance of the point $(x,y,z)$ from the surface $\mathcal{S}$, i.e. $d(\bar{x}, \mathcal{S}) = \min_{\bar{x}_s \in \mathcal{S}}\{\|\bar{x} - \bar{x}_s\|\}$, and $h(dist)$ is a penalty function that gets a constant low value when the distances are within the 'normal' range and grows fast otherwise, see Figure 1.

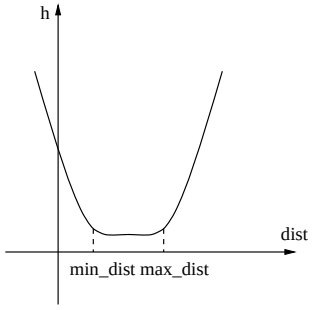


**Figure 1. The '$h$' function gets low constant value in the normal range**

It is clear that the minimum of the functional (3) is reached when both surfaces are located at their corresponding cortex boundaries and the inter-surface distance is preferably kept within the normal range.

## 2.2. Level set formulation

The Osher-Sethian [22] level set method is a numerical technique for analyzing evolving interface motion that works on a fixed coordinate system and considers an evolving front in an implicit form

$$\mathcal{S} = \{(x, y, z) | \Phi(x, y, z) = 0\}.$$

The basic idea is to evolve the three-dimensional embedding function $\Phi : \mathbb{R}^3 \rightarrow \mathbb{R}$ so that its zero level set would always track the current position of the evolving surface $\mathcal{S}$. Let us denote the set of 2D surfaces defined by different level sets of $\Phi$ by $\mathcal{S}(u, v, \phi)$. Then, the original surface is defined as $\mathcal{S}(u, v) = \mathcal{S}(u, v, \phi)|_{\phi=0}$.

Using the Coarea equation [12] one can prove that close to the interface

$$\begin{aligned}
&\iiint_{\phi\, u\, v} h\left[d(\mathcal{S}^{in}(u,v,\phi), \mathcal{S}^{out})\right] g_{in}(\mathcal{S}^{in}(u,v,\phi)) \\
&\qquad \cdot |\mathcal{S}^{in}_u \times \mathcal{S}^{in}_v| du dv d\phi + \\
&\iiint_{\phi\, u\, v} h\left[d(\mathcal{S}^{out}(u,v,\phi), \mathcal{S}^{in})\right] g_{out}(\mathcal{S}^{out}(u,v,\phi)) \\
&\qquad \cdot |\mathcal{S}^{out}_u \times \mathcal{S}^{out}_v| du dv d\phi \\
&= \iiint_{x\, y\, z} h\left[d((x,y,z), \mathcal{S}^{out})\right] g_{in}(x,y,z) |\nabla \Phi^{in}| dx dy dz + \\
&\iiint_{x\, y\, z} h\left[d((x,y,z), \mathcal{S}^{in})\right] g_{out}(x,y,z)) |\nabla \Phi^{out}| dx dy dz.
\end{aligned} \tag{4}$$

Essentially, Equation (4) enables us to implement surface evolution on the fixed $x, y, z$ coordinate system. Besides its important property of automatic handling topological changes of the evolving surface, the level set approach gives us a very simple and stable way to compute the distance used as an argument of the $h$ function. Since the implicit representation of the evolving surface does not imply any restrictions on the form of the embedding function, we are free to define the $\Phi$ function as a distance map. Then, the distance from a point $(x, y, z)$ to the surface $\mathcal{S}$, defined by the zero level set of the embedding function $\Phi$, is simply $\Phi(x, y, z)$. Therefore, the expression in (4) can be rewritten as

$$\begin{aligned}
&\mathcal{L}(\Phi^{in}, \Phi^{out}) = \\
&\qquad \iiint_{x\, y\, z} h(\Phi^{out}(x,y,z)) g_{in}(x,y,z) |\nabla \Phi^{in}| dx dy dz + \\
&\qquad \iiint_{x\, y\, z} h(\Phi^{in}(x,y,z)) g_{out}(x,y,z)) |\nabla \Phi^{out}| dx dy dz,
\end{aligned} \tag{5}$$

subject to $\Phi^{in}$ and $\Phi^{out}$ are distance extensions from their zero sets, and we are looking for $\left(\Phi^{in}, \Phi^{out}\right) = \arg\min_{\Phi^{in}, \Phi^{out}} \mathcal{L}(\Phi^{in}, \Phi^{out})$.

Taking the variation with respect to $\Phi^{in}$ and $\Phi^{out}$ and writing it as a gradient descent flow yields the system

$$\begin{aligned}
\frac{d\Phi^{in}}{dt} &= \text{div}\left[h(\Phi^{out}) g_{in}(x,y,z) \frac{\nabla \Phi^{in}}{|\nabla \Phi^{in}|}\right] + \\
&\qquad \frac{dh(\Phi^{in})}{d\Phi^{in}} g_{out}(x,y,z) |\nabla \Phi^{out}| \\
\frac{d\Phi^{out}}{dt} &= \text{div}\left[h(\Phi^{in}) g_{out}(x,y,z) \frac{\nabla \Phi^{out}}{|\nabla \Phi^{out}|}\right] + \\
&\qquad \frac{dh(\Phi^{out})}{d\Phi^{out}} g_{in}(x,y,z) |\nabla \Phi^{in}|.
\end{aligned} \tag{6}$$

There exists one limitation to the model developed so far. As the system uses only local information, it can be trapped by a meaningless local minimum, unless initialized close to the desired boundary. In order to overcome this difficulty we add an additional force that comes from volume maximization and is known as the balloon force [9]. We add the following volume maximization terms to the functional

$$\begin{aligned}
\alpha \left[\int_{\mathcal{S}^{in}} dV + \int_{\mathcal{S}^{out}} dV\right] &= \alpha \left[\iint_{u\, v} \mathcal{S}^{in} \cdot \left(\mathcal{S}^{in}_u \times \mathcal{S}^{in}_v\right) du dv + \right. \\
&\qquad \left. \iint_{u\, v} \mathcal{S}^{out} \cdot \left(\mathcal{S}^{out}_u \times \mathcal{S}^{out}_v\right) du dv \right],
\end{aligned} \tag{7}$$

where $dV$ is a volume element and $\alpha$ is a negative constant. It is equivalent to applying a pressure force outward. In order to stop the surface expansion near the desired boundary we also multiply the propagation forces by the edge indicator function (using the freedom of parameterization of the gradient descent). In level set formulation this yields

$$\begin{aligned}
\frac{d\Phi^{in}}{dt} &= g_{in} \cdot \left(\text{div}\left[h(\Phi^{out}) g_{in} \frac{\nabla \Phi^{in}}{|\nabla \Phi^{in}|}\right] + \right. \\
&\qquad \left. \frac{dh(\Phi^{in})}{d\Phi^{in}} g_{out} |\nabla \Phi^{out}| + \alpha |\nabla \Phi^{in}| \right) \\
\frac{d\Phi^{out}}{dt} &= g_{out} \cdot \left(\text{div}\left[h(\Phi^{in}) g_{out} \frac{\nabla \Phi^{out}}{|\nabla \Phi^{out}|}\right] + \right. \\
&\qquad \left. \frac{dh(\Phi^{out})}{d\Phi^{out}} g_{in} |\nabla \Phi^{in}| + \alpha |\nabla \Phi^{out}| \right).
\end{aligned} \tag{8}$$

## 2.3. Numerical scheme

An explicit Euler scheme with forward time derivative introduces a numerical limitation on the time step needed for stability. Moreover, the whole domain needs to be updated each step, which is a time consuming operation.

In order to cope with these limitations we use the fast geodesic active contours approach [13] which is based on the Weickert-Romeny-Viergever [32] semi-implicit additive operator splitting (AOS) scheme and uses the narrow band approach to limit the computation to a tight region of few grid points around the zero level set [7, 1].

We rely on the fact that the embedding function $\Phi$ is a distance map. Gomes and Faugeras [14] proposed an approach, where the Hamilton-Jacobi equation used to evolve the distance function is replaced by a PDE that preserves the $\Phi$ function as a distance map (see also [28]), which was applied for cortex segmentation using the coupled surfaces model, see also [33]. Here we re-initialize the $\Phi$ function every iteration using the fast marching method [26, 25, 31], which is a computationally optimal numerical method for distance computation on rectangular grids. The method has a computational complexity bound of $O(N)$, where $N$ is the number of points in the narrow band as shown by Tsitsiklis [31], and requires a set of grid points with a known exact distance to the zero level set for initialization. Those seed points are detected with sub-pixel accuracy using an algorithm motivated by the 'Marching Cubes' algorithm [17, 8]. For every grid cube within the narrow band where the $\Phi$ function changes its sign we find the distance to the zero level set for each one of the eight cube vertices. The cube is split into five pyramids (Figure 2(a)) and within each pyramid the $\Phi$ function is approximated by a four-dimensional hyperplane.

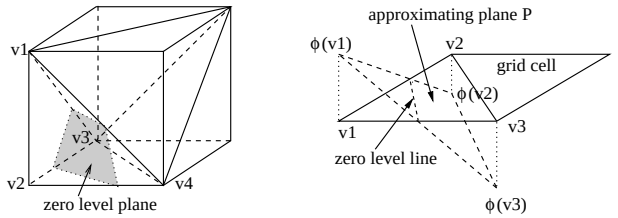


**Figure 2. (a) Grid cube split into five pyramids (b) Finding distance to the zero level curve - 2D case**

In order to clarify this idea let us first explore the low dimensional case where a 2D curve is implicitly given by the zero level of a function $\Phi : \mathbb{R}^2 \rightarrow \mathbb{R}$ (Figure 2(b)). A grid cell is split into two triangles and there exists one and only one plane, $P$, going through the points $\Phi(v_1), \Phi(v_2)$ and $\Phi(v_3)$, where $v_1$, $v_2$ and $v_3$ are the triangle vertices. The values of the $\Phi$ function at the vertices are then updated to the distance between the vertex and the zero level line of $P$. Each vertex adopts the minimal of all its updates.

Going back to the three-dimensional case, let $\bar{n}_{4\times 1}$ be a vector defining a hyperplane in 4D going through the four points $\Phi(v_1)$, $\Phi(v_2)$, $\Phi(v_3)$ and $\Phi(v_4)$ (Figure 2(a)), so that the hyperplane equation is given by $\bar{n}^T\bar{x} = \Phi$, where $\bar{x}$ is a 3D point written in homogeneous coordinates. The plane $\bar{n}$ can be found by solving the system of four linear equations $\{\bar{n}^T\bar{v_i} = \Phi(v_i), i = 1, .., 4\}$. Then, the zero level set of hyperplane $\bar{n}$ is a plane in 3D given by $\bar{n}^T\bar{x} = 0$. The distances we are looking for are the distances from vertices $v_i$ to the zero level plane. One should verify that the normal vector from the $v_i$ to the zero level plane is inside the pyramid. Otherwise, the shortest distance on the intersection of the plane with the pyramid boundary is taken instead.

The procedure above is repeated each iteration for both inner and outer surfaces and the corresponding narrow bands automatically modify their shapes as we re-initialize the distance maps. As one can see from (6), when updating $\Phi^{in}$ the values of $\Phi^{out}$ are to be defined within the area of $\Phi^{in}$ numerical support, and vice a versa. Therefore, it is important to ensure that the narrow band of one surface includes the other. This can be done using asymmetric narrow bands as in [33], or using a single narrow band for both surfaces.

## 3. Experimental Results

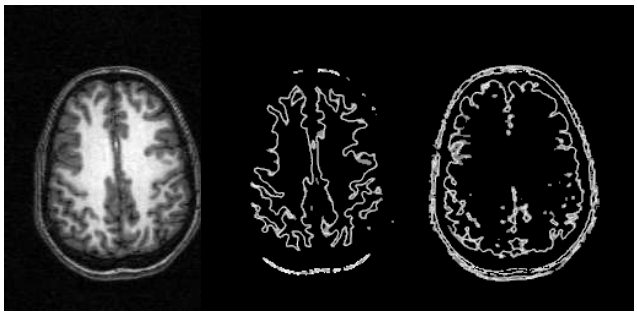

(a) (b) (c)

**Figure 3. Boundary indicator functions: (a) A slice from the original MR image. (b) Result of the inner boundary detection operator. (c) Result of the outer boundary detection operator**

In order to apply our method to cortex segmentation we have yet to determine appropriate boundary indicator functions for the inner and outer interfaces: $g_{in}$ and $g_{out}$. Here, we adopt a simplified version of an operator used by Zeng et al. [33], measuring the likelihood of a voxel to be on the boundary between two tissues. It is assumed that a statistical distribution of the image intensities is known for each one of the three tissues (CSF, gray matter, and white matter).

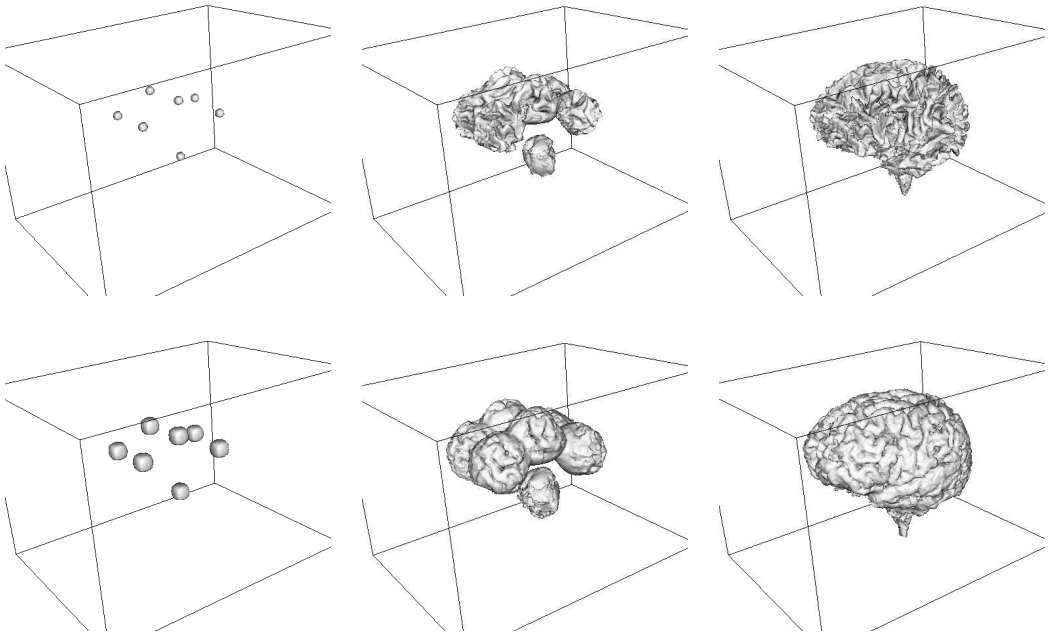

(a) (b) (c)

**Figure 4. Coupled surfaces propagation. Top: inner surface, Bottom: outer surface. (a) Initial position, (b) Intermediate state, (c) Final result.**

The probability of a voxel $v$ to be on the boundary between tissue A and tissue B is estimated from the ratio between the probability measures integrated over a neighborhood of $v$. Figure 3 shows the result of applying the inner and outer boundary detectors on a single slice from the original MR brain image.

We still need to set initial conditions (the initial position of the surfaces) in order to start the segmentation process. This is done by manually choosing several seed points inside the white matter region and building two small concentric surfaces (e.g. spheres or cubes) at the normal distance from each other. Figure 4(a) shows an initial condition with seven 'seeds'.

The coupled surfaces then propagate outwards, driven by a balloon force multiplied by the boundary indicator function, while maintaining the inter-surface distance, which is controlled by the $h$ function (3). Finally, the interfaces converge to their exact boundary position that minimize the weighted area and maximal volume as determined by the functionals (4) and (7). The process terminates when the surfaces do not change for two time steps. Figures 4(b,c) show an intermediate state and the final result. Both inner and outer surfaces are shown.

The three standard views (sagittal, axial and coronal) of the segmented outer and inner cortical surfaces are presented in Figure 5 and a zoom-in of the extracted boundaries for a single slice is shown in Figure 6.

For a 192x250x170 MR image of the whole brain, our algorithm runs in about 2.5 minutes on a Pentium III PC.

## 4. Concluding remarks

In this paper we presented a new approach for cortex segmentation. The method is based on the coupled surfaces model that was derived as a minimization problem in a variational geometric framework. The surface evolution is performed using the fast geodesic active contour approach - an efficient numerical scheme combining semi-implicit additive operator splitting propagation scheme, level set representation, narrow band approach and the fast marching method. An efficient technique is proposed for the zero level set reconstruction in 3D. Cortex segmentation results from a real MR brain images were presented.

## 5. Acknowledgements

We thank Prof. Gabriele Lohmann from Max Planck Institute of Cognitive Neuroscience who kindly provided us with the brain MR images. This research was partially supported by the German-Israeli Foundation (GIF).

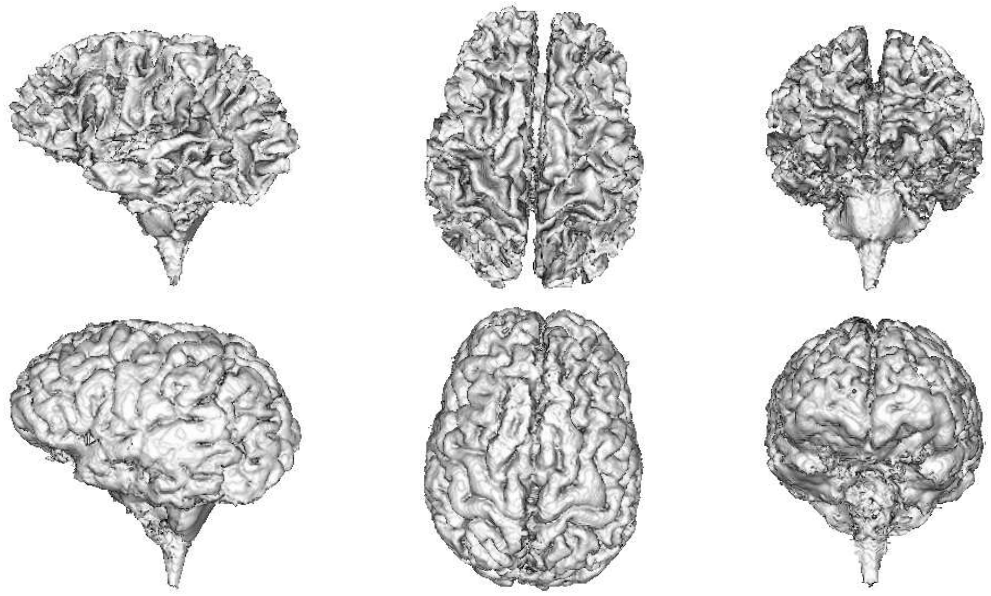

(a) (b) (c)

**Figure 5. Different views of the reconstructed cortical surfaces. Top: Inner surface. Bottom: Outer surface. (a) Sagittal view, (b) Axial view, (c) Coronal view.**

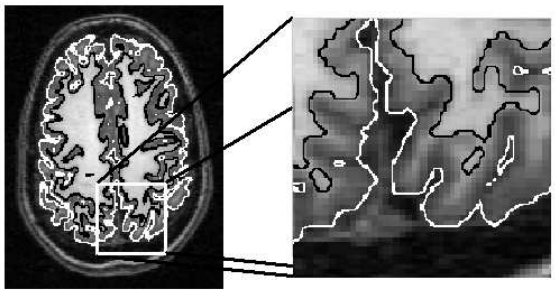

**Figure 6. Extracted boundaries in a single slice section and a zoom into a small region. White contour - outer surface, black contour - inner surface**

## References


[1] D. Adalsteinsson and J. A. Sethian. A fast level set method for propagating interfaces. *J. of Comp. Phys.*, 118:269–277, 1995.

[2] S. M. Blinkov and I. I. Glezer. *The Human Brain In Figures and Tables, A Quantative Handbook.* Plenum, New York, 1968.

[3] V. Caselles, F. Catte, T. Coll, and F. Dibos. A geometric model for active contours. *Numerische Mathematik*, 66:1–31, 1993.

[4] V. Caselles, R. Kimmel, and G. Sapiro. Geodesic active contours. In *Proceedings ICCV'95*, pages 694–699, Boston, Massachusetts, June 1995.

[5] V. Caselles, R. Kimmel, and G. Sapiro. Geodesic active contours. *IJCV*, 22(1):61–79, 1997.

[6] T. Chan and L. Vese. An active contour model without edges. *Scale-space theories in computer vision, Lecture Notes in Computer Science*, 1682:141–151, 1999. M. Nielsen, P. Johansen, O.F. Olsen, J. Weickert (Eds.).

[7] D. L. Chopp. Computing minimal surfaces via level set curvature flow. *J. of Computational Physics*, 106(1):77–91, May 1993.

[8] H. E. Cline, W. E. Lorensen, R. Kikinis, and F. Jolesz. Three-dimensional segmentation of MR images of the head using probability and connectivity. *Journal of Computer Assisted Tomography*, 14(6):1037–1045, 1990.

[9] L. D. Cohen. On active contour models and balloons. *CVGIP: Image Understanding*, 53(2):211–218, 1991.

[10] C. A. Davatzikos and R. N. Bryan. Using a deformable surface model to obtain a shape representation of the cortex. *IEEE Trans. Med. Imag.*, 15:785–795, 1996.

[11] C. A. Davatzikos and J. Prince. An active contour model for mapping the cortex. *IEEE Trans. Med. Imag.*, 14:65–80, 1995.

[12] L. C. Evans and R. F. Gariepy. *Measure theory and fine properties of functions.* CRC Press, 1992.

[13] R. Goldenberg, R. Kimmel, E. Rivlin, and M. Rudzsky. Fast geodesic active contours. *Scale-space theories in com-*

*puter vision, Lecture Notes in Computer Science*, 1682:34–45, 1999. M. Nielsen, P. Johansen, O.F. Olsen, J. Weickert (Eds.).

[14] J. Gomes and O. Faugeras. Reconciling distance functions and level sets. *Scale-space theories in computer vision, Lecture Notes in Computer Science*, 1682:70–81, 1999. M. Nielsen, P. Johansen, O.F. Olsen, J. Weickert (Eds.).

[15] M. Kass, A. Witkin, and D. Terzopoulos. Snakes: Active contour models. *International Journal of Computer Vision*, 1:321–331, 1988.

[16] S. Kichenassamy, A. Kumar, P. Olver, A. Tannenbaum, and A. Yezzi. Gradient flows and geometric active contour models. In *Proceedings ICCV'95*, Boston, Massachusetts, June 1995.

[17] W. E. Lorensen and H. E. Cline. Marching cubes: A high resolution 3d surface construction algorithm. *ACM Computer Graphics*, 21(24):163–169, July 1987.

[18] D. MacDonald, D. Avis, and A. E. Evans. Multiple surface identification and matching in magnetic resonance images. *Proc. SPIE*, 2359:160–169, 1994.

[19] D. MacDonald, D. Avis, and A. E. Evans. Proximity constraints in deformable models for cortical surface. In *Proc. First Int. Conf. Medical Image Computing Computer-Assisted Intervention*, pages 650–659, Boston, MA, 1998.

[20] R. Malladi and J. A. Sethian. An O(N log N) algorithm for shape modeling. *Proceedings of National Academy of Sciences, USA*, 93:9389–9392, 1996.

[21] R. Malladi, J. A. Sethian, and B. C. Vemuri. Shape modeling with front propagation: A level set approach. *IEEE Trans. on PAMI*, 17:158–175, 1995.

[22] S. J. Osher and J. A. Sethian. Fronts propagating with curvature dependent speed: Algorithms based on Hamilton-Jacobi formulations. *J. of Comp. Phys.*, 79:12–49, 1988.

[23] N. Paragios and R. Deriche. Coupled geodesic active regions for image segmentation. In *European Conference in Computer Vision*, Dublin, Ireland, 2000.

[24] C. Samson, L. Blanc-Feraud, G. Aubert, and J. Zerubia. A level set model for image classification. In *Intl. Conf. on Scale-space theories in computer vision*, pages 306–317, 1999.

[25] J. A. Sethian. *Level Set Methods: Evolving Interfaces in Geometry, Fluid Mechanics, Computer Vision and Materials Sciences*. Cambridge Univ. Press, 1996.

[26] J. A. Sethian. A marching level set method for monotonically advancing fronts. *Proc. Nat. Acad. Sci.*, 93(4), 1996.

[27] J. Shah. A common framework for curve evolution, segmentation and anisotropic diffusion. In *Proceedings IEEE CVPR'96*, pages 136–142, 1996.

[28] A. Steiner, R. Kimmel, and A. M. Bruckstein. Shape enhancement and exaggeration. *Graphical Models and Image Processing*, 60(2):112–124, 1998.

[29] P. C. Teo, G. Sapiro, and B. Wandell. Creating connected representations of cortical gray matter for functional MRI visualization. *IEEE Trans. on Medical Imaging*, 16:852–863, 1997.

[30] D. Terzopoulos, A. Witkin, and M. Kass. Constraints on deformable models: Recovering 3d shape and nonrigid motions. *Artificial Intelligence*, 36:91–123, 1988.

[31] J. N. Tsitsiklis. Efficient algorithms for globally optimal trajectories. *IEEE Trans. on Automatic Control*, 40(9):1528–1538, 1995.

[32] J. Weickert, B. M. t. Romeny, and M. A. Viergever. Efficient and reliable scheme for nonlinear diffusion filtering. *IEEE Trans. on Image Processing*, 7(3):398–410, 1998.

[33] X. Zeng, L. H. Staib, R. T. Schultz, and J. S. Duncan. Segmentation and measurement of the cortex from 3D MR images using coupled surfaces propagation. *IEEE Transactions on Medical Imaging*, pages 100–111, October 1999.